Thermodynamics of Portland Cement Clinkering

Theodore Hanein[1], Fredrik P. Glasser[2], Marcus Bannerman[1*]
1. School of Engineering, University of Aberdeen, AB24 3UE, United Kingdom
2. Department of Chemistry, University of Aberdeen, AB24 3UE, United Kingdom

Abstract
The useful properties of cement arise from the assemblage of solid phases present within the cement clinker. The phase proportions produced from a given feedstock are often predicted using well-established stoichiometric relations, such as the Bogue equations. These approaches are based on a single estimation of the stable phases produced under standard processing conditions and so they are limited in their general application. This work presents a thermodynamic database and simple equilibrium model which is capable of predicting cement phase stability across the full range of kiln temperatures, including the effect of atmospheric conditions. This is termed a "reaction path" and benchmarks the kinetics of processes occurring in the kiln. Phase stability is calculated using stoichiometric phase data and Gibbs free energy minimization under the constraints of an elemental balance. Predictions of stable phases and standard phase diagrams are reproduced for the manufacture of ordinary Portland cement and validated against results in the literature. The stability of low-temperature phases, which may be important in kiln operation, is explored. Finally, an outlook on future applications of the database in optimizing cement plant operation and development of new cement formulations is provided.

Originality
This report details corrections to reference thermodynamic data which are relevant for cement thermodynamic calculations. When combined with a suitable thermodynamic model, this data allows the calculation of the stable cement clinker phases across a range of feedstock compositions, operating conditions, and atmospheres. Here we present updated calculations of standard cement processing phase diagrams and data. In comparison to other studies, this work includes greater numbers of components and a more comprehensive database, revealing solid-gas reactions and the early-stage formation of phases such as spurrite (C_5S_2C') whose importance may not be fully appreciated. The accuracy of the predictions demonstrates that a stoichiometric approach is useful even at the highest kiln temperatures. The database also includes enthalpic data which can be used as the basis of a process and heat transfer model to optimize and design entire cement production processes.

Keywords*: Cement; Thermodynamics; Clinker phases, High temperature.*

*** Corresponding author: m.campbellbannerman@abdn.ac.uk, Tel +44-1224-27-4480**

1 Introduction

The thermodynamics of cement chemistry have long been studied and were first applied by Le Chatelier in 1905 (Le Chatelier, 1905). Much of the published literature has focused on cement hydration (Damidot et al., 2011) where the collection of thermodynamic data is typically focused on temperatures in the range of 0—100°C. However, the useful properties of cement arise from the assemblage of solid phases which are produced within the kiln at temperatures of up to 1500°C (Taylor, 1997). Numerous thermodynamic models have been developed for calculating equilibrium over this temperature range, including MTDATA (Davies et al., 2002), FactSage (Bale et al., 2002), and HSC (Roine, 2002). Solid solution models are often used to correlate the properties of complex solid phases: however, it is not straightforward to repurpose existing models as they are often parameterized for applications other than cement chemistry. Extensive process calculations, especially heat balances, are normally not possible with solid solution models as in almost all cases a simple linear temperature dependence is assumed (Hack, 2008). There is also a relative lack of studies into high-temperature thermodynamic data and models for pure phases involved in cement production, although there are notable exceptions: e.g., see Haas Jr et al., 1981.

In practice, the estimation of the proportionality of clinker phases produced from a given feedstock is often predicted using well-established stoichiometric relations, such as the Bogue equations (Bogue, 1929). These are based on a single estimation of the stable phases in OPC at the solidus temperature of the assemblage C_3S-C_3A-C_2S-ferrite and, without a more fundamental thermodynamic description; they cannot be used to predict the evolution of phases across changes in temperature and atmospheres, or be applied to novel cement formulations.

Tab. 1 Cement Chemistry Notation used in this work.

Oxide	CaO	SiO_2	Al_2O_3	Fe_2O_3	K_2O	MgO	Na_2O	SO_3	CO_2	TiO_2
Notation	C	S	A	F	K	M	N	S’	C’	T

High temperature cement phase equilibrium has been used to understand clinker reactions as shown by Barry and Glasser (Barry & Glasser, 2000) who indicate that assumptions underlying the Bogue calculation do not provide a completely satisfactory basis for clinker phase estimation. In their work, they have used both stoichiometric compounds and solid-phase solution models at temperatures greater than 1200°C and focused on the consequences to phase amounts of Scheil cooling (Scheil, 1942) on the C-F-A-S equilibria (see table 1 for notation). They were also limited by the thermodynamic data available in MTDATA.

Hökfors et al. (Hökfors et al., 2014) have developed a more advanced thermodynamic equilibrium model for predicting the chemistry of clinker. The basis of this is a solid solution model using thermodynamic data from FactSage; however, the database lacks data for various important compounds formed below clinker solidus temperatures, such as spurrite. The predictions of Hökfors et al. are compared to those presented in this work in the validation section.

Ghanbari Ahari et al. (Ghanbari Ahari et al., 2004) have also used both FactSage and MTDATA to carry out high temperature thermodynamic equilibrium calculations on 4 (C, F, A, and S), 5 (C, F, A, S, and M), and 7 (C, F, A, S, M, N, and K), component systems using both stoichiometric compounds and solution models. Scheil cooling calculations were also carried out to simulate the effects of a melt phase which, upon cooling, solidifies by a peritectic reaction. Their 7-component system considered alkali oxides but failed to consider the S’ component, which will result in inaccurate predictions as the formation of alkali sulfate liquid and vapours are important to the OPC manufacture process.

The thermodynamic calculations carried out in this work are intended to explore what happens as the clinker batch is heated. Broadly we accept that, using present knowledge, batch components can be characterised and that we can calculate with reasonable accuracy the final products. But the reaction path: the way we progress from raw meals to clinker, is what we seek to define in this title study.

Calculations are based on data compiled and harmonized from various publications, the full listing of each considered species and the data source is given in tables 2 and 3. The title study is based on a 10 oxide component system, namely, C, S, A, F, M, K, N, T, S’, and C’. All phases are treated as stoichiometric compounds as this simplifies the approach and allows calculations directly on the experimentally determined thermodynamic data. This simple approach means that melt phases are not yet included and the implications of this are discussed subsequently. In attempting to compile a comprehensive thermodynamic database of stoichiometric cement clinker phases and in the

production of a model for high temperature clinker phase predictions, a significant number of misprints and errors in published coefficients were found in the literature. The data sources used and these errors are discussed in the following section.

2 Data and sources

Thermodynamic data for gas phases and a number of liquids and solids have been taken from the NASA CEA database (McBride et al., 2002). This is a comprehensive and freely available data set originally used in rocket combustion calculations; therefore it is ideally suited for modelling atmospheric reactions under kiln conditions. Data for many of the major clinker solid phases have been obtained from the benchmark study by Haas Jr et al. (Haas Jr et al., 1981); however it contains a number of misprints in the enthalpy constant (a_2) as detailed in table 2. These data were checked and corrected by considering the tables of calculated data for each species given in the reference. There are a number of key phases which are not included in the above references. The compilation of Babushkin et al. (Babushkin et al., 1985) is another source of thermodynamic data; however, numerous transcription errors are also present in this compilation. For example, the heat capacity coefficients for C_3A differ to those in the original source and these errors have even been carried over into the CEMDATA07 database used in GEMS (Thoenen & Kulik, 2003). To reduce transcription errors, the heat capacity data used in this work are taken directly from the original sources. Reference enthalpy and entropy constants were generally taken from the NBS tables (Wagman et al., 1982). Some of the literature sources listed here contain differing data for the same species. In these cases the sources are favoured in the following order (McBride et al., 2002), (Haas Jr et al., 1981), (Holland & Powell, 2011), (Wagman et al., 1982), and (Bard et al., 1985). One limitation of the present data is that hatrurite and other polymorphs of C_3S are undifferentiated as available data are insufficient to evaluate properties of the individual polymorphs. The data used in the title study therefore represent the average properties of all polymorphs (Haas Jr et al., 1981).

Tab. 2 Species considered in this work whose thermodynamic data come from a single source. Values given in braces ({X}) are the number of polymorphs available in the database.

Source	Phase	Species
(McBride et al., 2002)	Gases	Ar, C_2, C_2H_4, C_3OS, CH, CH_2, CH_3, CH_4, CN, CO, CO_2, COS, H, H_2, H_2O, H_2SO_4, HCN, HCO, HO_2, He, K, K_2SO_4, KOH, Kr, N, N_2, N_2O, NH, NH_2, NH_3, NO, Na, Na_2SO_4, NaOH, Ne, O, O_2, OH, S_2O, SO_2, SO_3, SO, CO_2^+, NO^+, H_3O^+, NO_3^-, NO_2^-, OH^+, HCO^+, OH^-, $CaOH^+$, O_2^+, H_2O^+, Al_2O^+, $Al_2O_2^+$, CO^+, TiO^+, AlO_2^-, SO_2^-, O_2^-, Na_2O, CH_2OH^+, O^+, $MgOH^+$, CaO^+, AlO^-, $N2O^+$, $NaOH^+$, AlO^+, HO_2^-, K_2O^+
	Liquids	H_2O, $MgCO_3$, Na_2CO_3, Na_2O, K_2O, Na_2SO_4, K_2CO_3, K_2SO_4, $K_2Si_2O_5$, K_2SiO_3, $MgSiO_3$, $CaSO_4$, $CaCO_3$
	Solids	$CaCO_3$, Mg_2SiO_4, Fe_2O_3 {2}, $MgCO_3$, $KAlO_2$, Na_2CO_3 {3}, $NaAlO_2$ {2}, Na_2O {3}, K_2O {3}, Na_2SO_4 {3}, K_2CO_3 {2}, K_2SO_4 {2}, $K_2Si_2O_5$ {3}, K_2SiO_3, $MgSiO_3$ {3}, MgO, $CaSO_4$ {2}, $MgTiO_3$, Mg_2TiO_4, $MgTi_2O_5$, Ti_3O_5 {2}, TiO_2, TiO {3}, Ti_2O_3 {2}, Ti_4O_7
(Haas Jr et al., 1981)	Solids	$HAlO_2$[a] {2}, $Al(OH)_3$, $CaAl_2SiO_6$, $CaAl_2Si_2O_8$, $Ca_2Al_2Si_3O_{10}(OH)_2$[b], $Ca_2Al_2SiO_7$, $Ca_3Al_2Si_3O_{12}$, $Al_2Si_4O_{10}(OH)_2$, $Al_2Si_2O_5(OH)_4$ {3}, Al_2O_3, Al_2SiO_5 {3}, $Ca_2Al_3Si_3O_{12}(OH)$[c], $CaAl_4Si_2O_{10}(OH)_2$[d], CaO, $CaSiO_3$ {2}, Ca_2SiO_4 {4}, Ca_3SiO_5, $Ca_3Si_2O_7$, SiO_2 {2}
(Holland & Powell, 2011)	Liquids	$NaAlSi_3O_8$, $CaAl_2Si_2O_8$, $CaMgSi_2O_6$, $Mg_2Si_2O_6$, Fe_2SiO_4, Mg_2SiO_4, $KAlSi_3O_8$, Al_2SiO_5
	Solids	$Ca_5Si_2CO_{11}$, $CaMgC_2O_6$, $Ca_5Si_2C_2O_{13}$, $NaAlSi_3O_8$ {2}, $CaMgSi_2O_6$, $Mg_2Si_2O_6$, $KAlSi_3O_8$, $NaAlSi_2O_6$, $NaFeSi_2O_6$, Fe_2SiO_4, $Fe_2Si_2O_6$
(Waldbaum, 1965)	Solid	$Al_6Si_2O_{13}$

a) (Diaspore) constant (a_2) value corrected to 15671.57. b) (Prehnite) constant (a_2) value corrected to 96995.98159. c) (Zoisite) constant (a_2) value corrected to 34330.82985. d) (Margarite) constant (a_2) value corrected to 46846.59733.

Tab. 3 Species included in this work whose thermodynamic data are combined from multiple sources. Values given in braces ({X}) are the number of polymorphs available in the database.

	Source		
Solids	**(Cp)**	**(Hf^o)**	**(S^o)**
$Ca_3Al_2O_6$, $Ca_{12}Al_{14}O_{33}$ {2}, $CaAl_2O_4$, $CaAl_4O_7$, $MgAl_2O_4$	(Bonnickson, 1955)	(Wagman et al., 1982)	(Wagman et al., 1982)
TiS2 {2}	(Todd & Coughlin, 1952)	(O'Hare & Johnson, 1986)	(Todd & Coughlin, 1952)
$CaFe_2O_4$, $Ca_2Fe_2O_5$, $MgFe_2O_4$ {3}	(Bonnickson, 1954)	(Wagman et al., 1982)	(Wagman et al., 1982)
$FeTiO_3$	(Naylor & Cook, 1946)	(Bard et al., 1985)	(Shomate, 1946)
$CaTiO_3$ {2}	(Naylor & Cook, 1946)	(Wagman et al., 1982)	(Wagman et al., 1982)
Na_2TiO_3 {2}	(Naylor, 1945)	(Wagman et al., 1982)	(Wagman et al., 1982)
$CaTiSiO_5$	(King et al., 1954)	(Wagman et al., 1982)	(Wagman et al., 1982)
$Ca_4Fe_2Al_2O_{10}$	(Babushkin et al., 1985)	(Thorvaldson et al., 1938)	(Zhu et al., 2011)
Liquids			
$CaFe_2O_4$, $Ca_2Fe_2O_5$	(Bonnickson, 1954)	(Wagman et al., 1982)	(Wagman et al., 1982)
$FeTiO_3$	(Naylor & Cook, 1946)	(Bard et al., 1985)	(Shomate, 1946)
Na_2TiO_3	(Naylor, 1945)	(Wagman et al., 1982)	(Wagman et al., 1982)
$CaTiSiO_5$	(King et al., 1954)	(Wagman et al., 1982)	(Wagman et al., 1982)

3 Methodology

To calculate the clinker products resulting from a particular raw feedstock and processing environment we consider equilibria where the temperature and pressure are equal between all phases and the entropy is at a maximum. At constant temperature and pressure, the entropy is maximized when the Gibbs free energy is minimized. To calculate the Gibbs free energy, the kiln atmosphere is assumed to be a single ideal gas mixture at the reference pressure (1 bar) and each solid or liquid phase is assumed to be of negligible volume (PV terms are small) compared to the atmosphere. The liquid and solid phases are assumed to be stoichiometric and immiscible. To determine the phase compositions at equilibrium, a Gibbs free energy minimization is performed under the constraints of an elemental balance. An SLSQP optimizer (Perez et al., 2012) is used to perform the constrained minimization. The compiled database and software package used to perform these calculations can be found online[1].

The assumption of equilibrium implies that reaction kinetics are fast and that the system is well mixed and isothermal. The predictions of this model must therefore be treated with care when comparing to experimental results where these assumptions may not be realised. Relaxing these assumptions is difficult as not all chemical reactions occurring in cement production process are known and only limited kinetic data are available.

4 Validation

The thermodynamic data and model considered in this work are validated against the calculations carried out by Hökfors et al. (Hökfors et al., 2014). Their equilibrium calculations are performed at a temperature of 1360°C followed by Scheil cooling and their raw meal composition is given in table 4. In this section, the same raw meal and equilibrium temperature as those of Hökfors et al. are considered, although the species P_2O_5, ZnO, and Cl were neglected from the raw meal as data for these species are not available in our database. The initial atmospheric composition is the same as that used by Hökfors et al., which is 21% oxygen and 79% nitrogen; however, the atmospheric mass used in their calculations was not reported. In our study, the input mass of air is adjusted such that the evolution of CO_2 from the solids results in a maximum CO_2 atmospheric concentration of 25 mol%. This maximum concentration occurs at high temperatures as CO_2 evolves from the calcination of limestone. Typical kiln exit gas compositions are approximately 50% CO_2 but a lower concentration

[1] http://github.com/toastedcrumpets/PyChemEng

is used here as the atmospheric input used is not a fuel/air combustion mixture (does not contain CO_2). A second validation is performed against the predictions of the Bogue equations. The comparison of results is given in table 5.

From table 5, we can see that the results of the thermodynamic data collected in this work closely agree with the results from Hökfors et al. and the Bogue calculations. The Bogue weight percentage calculations do not add up to 100%; this is due to the raw meal containing species which are not accounted for in the general four-phase (C_3S, C_2S, C_3A, C_4AF) Bogue equations used to calculate the values in table 5. Although the model presented in this work does not take into account solid solutions or oxide melting in the process which occurs at 1338°C (Glasser et al., 2004), we can still deduce the final clinker products by assuming (as in the Bogue calculations) that there are no significant phase changes in the course of rapid cooling, other than polymorphic transformations which are isochemical. The agreement between the predictions appears to validate the use of a purely stoichiometric approach. This model improves on the predictions of Hökfors et al. by reproducing the proportions of C_3A and C_4AF predicted by the Bogue equations. The Bogue equations appear to be able to capture the output of the model in the validation case, but this is a well-studied limit. In the following section, the model is taken beyond the limitations of the Bogue equation and is used to study the clinker production process across its entire temperature range.

Tab. 4 Raw meal composition taken from Hökfors et al. (Hökfors et al., 2014).

Compound	CC'	S	A	F	M	K	N	S'	T	P_2O_5	Cl	ZnO
Raw meal wt(%)	77.36	13.73	2.93	1.84	1.83	0.85	0.14	1.08	0.15	0.02	0.06	0.01

Tab. 5 A comparison between results from this work and results from Hökfors et al.(Hökfors et al., 2014) and Bogue calculations with a raw feed as reported in table 4. Entries marked N/A imply that the model used does not report/include these components. (C-A-F) represents the sum of all the calcium aluminate ferrite solid solutions reported by Hökfors et al.(Hökfors et al., 2014).

Phase	Equilibrium products wt(%) (Hökfors et al., 2014)	Scheil cooled products wt(%) (Hökfors et al., 2014)	Bogue calculated products wt(%)	This work products wt(%)
C_3S	72.3	72.3	75.24	75.69
C_2S (stoichiometric)	N/A	N/A	2.94	3.22
C_2S (solid solution)	3.5	6.2	N/A	N/A
(C-A-F)	0	14.5	N/A	N/A
C_3A	N/A	N/A	7.04	7.13
C_4AF	N/A	N/A	8.49	8.58
M	2.3	3.0	N/A	2.8
CT	N/A	N/A	N/A	0.39
NS' (L)	N/A	N/A	N/A	0.33
KS' (L)	N/A	N/A	N/A	1.84
C	1.3	2.0	N/A	0
Salt melt	0.8	1.3	N/A	N/A
Oxide melt	19.7	0	N/A	N/A

5 Results and Discussion

To study the predictions of the model for a representative OPC plant, a raw input feed must be specified. The input used by Hökfors et al. and described in the previous section is not used here as we are unable to determine its source. The raw input feed presented in this section is based on real field data taken from Aldieb and Ibrahim (Aldieb & Ibrahim, 2010) as shown in table 6. The kiln atmospheric composition was not reported; therefore it was assumed to have been generated from the combustion of pure methane in 15% excess air. In order to evaluate the amount of fuel to input to the system, it is assumed that 60% of the CO_2 released by the process arises from calcination of limestone and 40% from the combustion of fuel. Using these values in a mass balance, an input atmospheric composition can be calculated and the input values thus derived are given in table 7. In this

simulation, it is assumed that all the calcium and magnesium which are input into the process are in the form of carbonates (as is typical for naturally sourced raw meal). These carbonates will calcine as temperature increases during the thermodynamic calculations and release additional CO_2 in to the kiln atmosphere.

Tab. 6 Raw meal composition for OPC taken from Aldieb and Ibrahim (Aldieb & Ibrahim, 2010).

Compound	CC'	S	A	F	MC'	K	N	S'
Feed wt(%)	76.09	14.43	3.90	2.27	2.28	0.9	0.09	0.1

Tab. 7 Input atmosphere used along with the raw meal composition in table 6 for the thermodynamic calculations.

Species	O_2	N_2	CO_2	H_2O
(g/g raw meal)	0.01021	0.9802	0.2232	0.1826

As a first test of our calculations, the clinker composition at the selected equilibrium temperature (1338°C) is predicted for the new raw feed and again compared to the Bogue calculations, as shown in table 8. Again the agreement is close, as may be expected for a traditional OPC process. Although the thermodynamic model produced in this work does not consider melting, it can correctly capture clinker phase stability below the solidus temperature, and this region is explored.

Tab. 8 Comparisons between the Bogue calculations and the calculated equilibrium products at 1338°C for a raw feed and atmosphere as reported in tables 6 and 7 respectively.

Phase	C_3S	C_2S	C_3A	C_4AF	M
Bogue calculated products wt(%)	52.48	23.96	9.93	10.56	N/A
Equilibrium products wt(%)	53.57	23.90	10.10	10.74	1.69

The clinker solid phases at equilibrium for the temperature range 500—1338°C are calculated and shown in figure 1. This calculation can be compared to the textbook diagram given in figure 2 which is an adapted qualitative diagram (Taylor, 1997) representing conventional wisdom and based on kiln observations and laboratory experiments. Our equilibrium model appears to reproduce the qualitative phase chemistry over the entire process temperature range but with higher resolution of the stable phases and their proportions. Also, our results (see figure 1) show the stability of a number of phases over the processing temperature which are not captured in previous phase diagrams: e.g. spurrite. Calculations are performed at intervals of 2°C, thus the stepped appearance of the boundaries of the phases is due to the discrete changes in stable phases and is not an artefact of the resolution of the calculations. However, the abrupt changes in the phase stability are more likely to be smooth, like those shown in figure 2, due to the effects of kinetics and the small changes in free energy driving the reactions near the transition temperature. In this work, the Gibbs free energy is minimised until the difference between iterations is less than 10^{-6}. This translates to 10^{-3} % by mass for each component.

Figures 1 and 2 do not cover the same temperature ranges but from observation, it is apparent that below the solidus temperature, the equilibrium phase development diverges strongly between them. The formation of spurrite (C_5S_2C') can be seen in the temperature range 600—870°C in figure 1 but to the author's knowledge this is the first time its extensive formation has been predicted from thermodynamic calculations. Spurrite appears as an early-formed reaction product of the raw materials in cement production where sulfates, fluorides, and chlorides act as mineralizers for spurrite formation (Bolio-Arceo & Glasser, 1990; Glasser, 1973). Its formation has been held responsible in some studies for clinker ring formation in kilns (Bolio-Arceo & Glasser, 1990). Spurrite has also been observed to form either by the reaction of calcium carbonate and silica directly, and or the reaction of belite, lime, and carbon dioxide. Its reported decomposition temperature is observed to be between 750°C – 900°C depending on CO_2 partial pressure (Bolio-Arceo & Glasser, 1990; Glasser, 1973) which is in agreement with the calculations here.

Another observation evident in the equilibrium calculations is the stability of MgO at high temperatures. Its physical and chemical stability at high temperatures is universally known. Our calculations probably overestimate the amount of free MgO because no allowance is made for its substitution into belite, alite, ferrite etc.

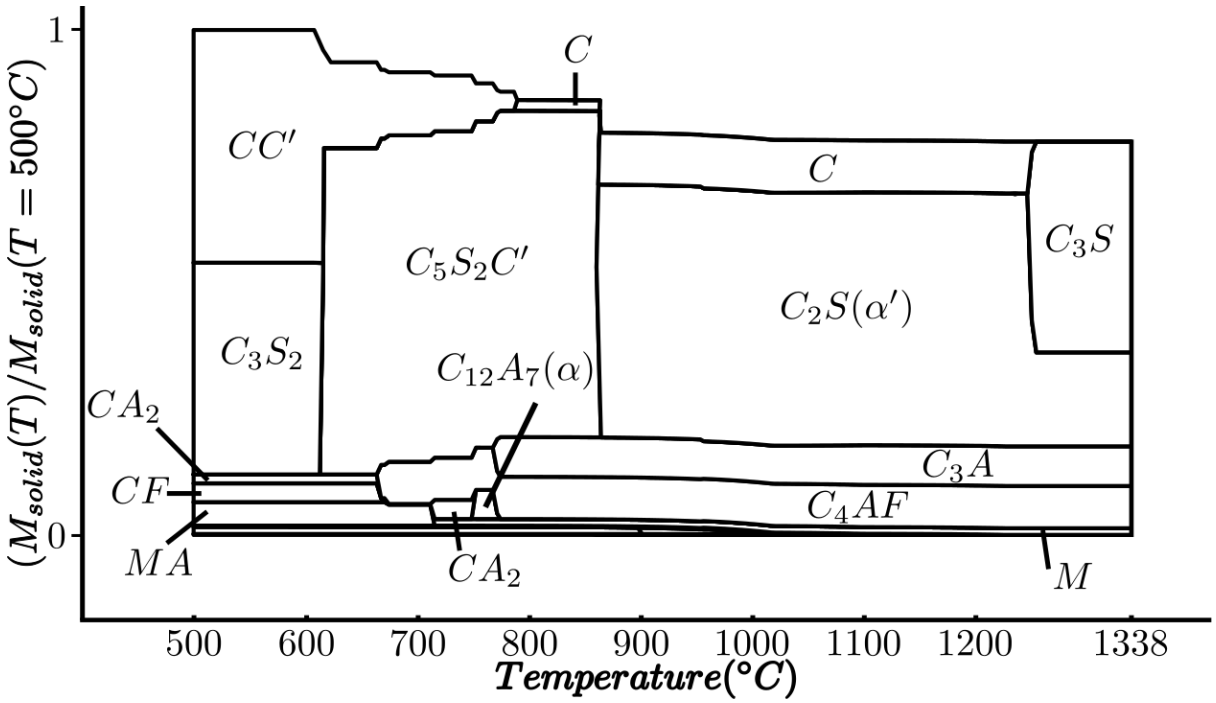

Figure 1 The equilibrium cumulative mass distribution of phases (relative to the solid mass at T=500°C) calculated for OPC clinker production over a range of temperatures. The raw feed and inlet atmospheric compositions are as reported in tables 6 and 7 respectively. Calculations are performed at intervals of 2°C.

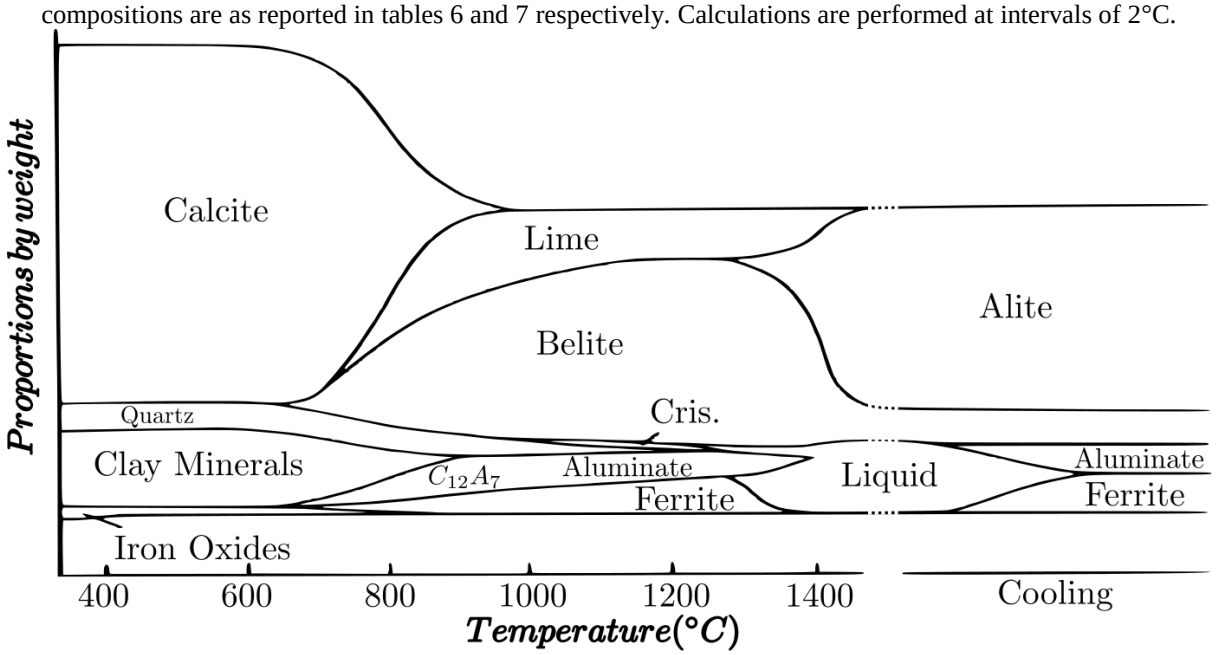

Figure 2 Variations in phases during the formation of OPC clinker. This figure is adapted from Taylor, 1997 and is a qualitative representation of the expected stable phases.

The minor phases forming in figure 1 relate to the formation and equilibrium of alkali sulfates and carbonates in both the solid and liquid state. As shown in the simulation calculations in section 4, the formation of liquid alkali sulfates is predicted in this work and can be justified as clinker phases are well known to contain alkali sulfates as partial fillings of pores in cement clinker (Campbell, 1986).

Research into the kinetics of reaction amongst solid phases has been neglected, partly due to the difficulty of assessing the influence of particle size, shape and packing. But another real difficulty has been to provide an equilibrium benchmark for the early-stage clinkering reactions. Thus most kinetic studies of clinkering below solidus temperatures assume that the benchmarks are set mainly by formation of C_2S, C_3A, C_4AF and C. C_3S is of course not included unless temperatures exceed ~1250°C because of its known instability at lower temperatures.

The present study shows that establishing an equilibrium benchmark for the kinetics is a much more complex task than first thought. The equilibrium path for clinkers undergoing steadily increasing temperature is marked by the formation of unexpected phases such as spurrite (C_5S_2S'), CA_2 and C_3S_2 (rankinite). The equilibrium path is also strongly controlled by the evolution of CO_2 gas from the raw materials. The evolution of CO_2 content with rising temperature, as shown in older studies (figure 2), represents a series of approximations based on what solids are observed to form, often by indirect observations, and it is possible that the real sequence in industrial scale kilns varies considerably from the generally accepted picture given in figure 2.

These variables, such as the evolution of solids and actual partial pressures of volatiles and their resulting impact on the reaction path, need to be investigated further. If the equilibrium phases predicted here are not obtained in the kiln, as well may be the case, the equilibrium information presented here is useful to elucidate and de-convolute both the kinetics of the competing reactions and the energy flows within the kiln.

6 Conclusions

The thermodynamic model allows us to calculate the stability of phases across the cement production process and can be used for the optimization of cement formulations as well as to study novel formulations. Its predictions below solidus temperatures are consistent with those made by the Bogue equations, but the data allows the consideration of lower-temperature phase stability. Spurrite also appears to be stable under low-temperature processing conditions and may inhibit attempts to make Portland clinkers using low melting point fluxed systems. The composition of the kiln atmosphere is shown to be an important variable controlling the sequence of reactions, the nature of the stable solids, and the reaction path for clinkers heated to progressively higher temperatures.

The database provides enthalpic data which can be used as the basis of a process model (as well as a heat transfer model) for optimization and design of entire cement production processes. These thermodynamic predictions can also be used as a benchmark for kinetic studies and the influence of time and mixing on the formation of clinker phases. Also, the database compiled contains thousands of other species and can be used with the produced package to simulate and optimize other high temperature systems.

This technique of clinker phase formation predictions has been validated for OPC production. Future work will compile and/or generate thermodynamic data for phases present in calcium sulfoaluminate and other alternative cement clinkers in order to predict and optimize their formulations and processing.

Acknowledgements

The authors would like to thank Gulf Organization for Research and Development (GORD, Qatar) for funding.

References

Aldieb, M. A., & Ibrahim, H. G. (2010). *Variation of feed chemical composition and its effect on clinker formation—simulation process*.

Babushkin, V. I., Matveev, G. M., & McHedlov-Petrosian, O. P. (1985). *Thermodynamics of silicates*: Springer-Verlag Berlin.

Bale, C. W., Chartrand, P., Degterov, S. A., Eriksson, G., Hack, K., Mahfoud, R. B., . . . Petersen, S. (2002). FactSage thermochemical software and databases. *Calphad, 26*(2), 189-228.

Bard, A. J., Parsons, R., & Jordan, J. (1985). *Standard potentials in aqueous solution* (Vol. 6): CRC press.

Barry, T. I., & Glasser, F. P. (2000). Calculations of Portland cement clinkering reactions. *Advances in cement research, 12*(1), 19-28.

Bogue, R. H. (1929). Calculation of the compounds in Portland cement. *Industrial & Engineering Chemistry Analytical Edition, 1*(4), 192-197.

Bolio-Arceo, H., & Glasser, F. P. (1990). Formation of spurrite, Ca5(SiO4)2CO3. *Cement and Concrete Research, 20*(2), 301-307.

Bonnickson, K. R. (1954). High temperature heat contents of calcium and magnesium ferrites. *Journal of the American Chemical Society, 76*(6), 1480-1482.

Bonnickson, K. R. (1955). High temperature heat contents of aluminates of calcium and magnesium. *The Journal of Physical Chemistry, 59*(3), 220-221.

Campbell, D. H. (1986). *Microscopical examination and interpretation of portland cement and clinker*: Construction Technology Laboratories.

Damidot, D., Lothenbach, B., Herfort, D., & Glasser, F. P. (2011). Thermodynamics and cement science. *Cement and Concrete Research, 41*(7), 679-695.

Davies, R. H., Dinsdale, A. T., Gisby, J. A., Robinson, J. A. J., & Martin, S. M. (2002). MTDATA - thermodynamic and phase equilibrium software from the national physical laboratory. *Calphad, 26*(2), 229-271. doi: citeulike-article-id:8982030 doi: 10.1016/s0364-5916(02)00036-6

Ghanbari Ahari, K., Thompson, D., Argent, B. B., & Sharp, J. H. (2004). Phase Equilibria Predictions by Computational Calculations on Portland Cement Clinker. *Key Engineering Materials, 264*, 2131-2136.

Glasser, F. P. (1973). The formation and thermal stability of spurrite, Ca5(SiO4)2CO3. *Cement and Concrete Research, 3*(1), 23-28.

Glasser, F. P., Bhatty, J. I., McGregor, F., & Kosmatka, S. H. (2004). Advances in Cement Clinkering. *Inovations in Portland Cement Manufacture*, 332.

Haas Jr, J. L., Robinson Jr, G. R., & Hemingway, B. S. (1981). Thermodynamic tabulations for selected phases in the system CaO-Al2O3-SiO2-H2 at 101.325 kPa (1 atm) between 273.15 and 1800 K. *Journal of Physical and Chemical Reference Data, 10*(3), 575-670.

Hack, K. (2008). *The SGTE casebook: thermodynamics at work*: Elsevier.

Holland, T. J. B., & Powell, R. (2011). An improved and extended internally consistent thermodynamic dataset for phases of petrological interest, involving a new equation of state for solids. *Journal of Metamorphic Geology, 29*(3), 333-383.

Hökfors, B., Boström, D., Viggh, E., & Backman, R. (2014). On the phase chemistry of Portland cement clinker.

King, E. G., Orr, R. L., & Bonnickson, K. R. (1954). Low temperature heat capacity, entropy at 298.16 K., and high temperature heat content of sphene (CaTiSiO5). *Journal of the American Chemical Society, 76*(17), 4320-4321.

Le Chatelier, H. (1905). *Experimental researches on the constitution of hydraulic mortars*: McGraw Publishing Company.

McBride, B. J., Zehe, M. J., & Gordon, S. (2002). *NASA Glenn coefficients for calculating thermodynamic properties of individual species*: National Aeronautics and Space Administration, John H. Glenn Research Center at Lewis Field.

Naylor, B. F. (1945). High-Temperature Heat Contents of Na2TiO3, Na2Ti2O5 and Na2Ti3O71. *Journal of the American Chemical Society, 67*(12), 2120-2122.

Naylor, B. F., & Cook, O. A. (1946). High-Temperature Heat Contents of the Metatitanates of Calcium, Iron and Magnesium1. *Journal of the American Chemical Society, 68*(6), 1003-1005. doi: 10.1021/ja01210a030

O'Hare, P. A. G., & Johnson, G. K. (1986). Thermochemistry of inorganic sulfur compounds VII. Standard molar enthalpy of formation at 298.15 K, high-temperature enthalpy increments, and other thermodynamic properties to 1100 K of titanium disulfide, TiS 2. *The Journal of Chemical Thermodynamics, 18*(2), 189-199.

Perez, R. E., Jansen, P. W., & Martins, J. R. R. A. (2012). pyOpt: a Python-based object-oriented framework for nonlinear constrained optimization. *Structural and Multidisciplinary Optimization, 45*(1), 101-118.

Roine, A. (2002). Outokumpu HSC chemistry for windows: chemical reaction and equilibrium software with extensive thermochemical database. *User's guide, version, 5*.

Scheil, E. (1942). Bemerkungen zur schichtkristallbildung. *Zeitschrift für Metallkunde, 34*(3), 70-72.

Shomate, C. H. (1946). Heat Capacities at Low Temperatures of the Metatitanates of Iron, Calcium and Magnesium1. *Journal of the American Chemical Society, 68*(6), 964-966. doi: 10.1021/ja01210a015

Taylor, H. F. W. (1997). Cement chemistry. *Telford, London*.

Thoenen, T., & Kulik, D. (2003). Nagra/PSI chemical thermodynamic data base 01/01 for the GEM-Selektor (V. 2-PSI) Geochemical Modeling Code: Release 28-02-03 *Technical Report, PSI Technical Report TM-44-03-04 about the GEMS Version of Nagra/PSI Chemical Thermodynamic Database 01/01*.

Thorvaldson, T., Edwards, R. R., & Bailey, E. C. (1938). Die Bildungswärme von Tetracalciumaluminiumferrit. *Zeitschrift für anorganische und allgemeine Chemie, 236*(1), 310-319.

Todd, S. S., & Coughlin, J. P. (1952). Low Temperature Heat Capacity, Entropy at 298.16° K. and High Temperature Heat Content of Titanium Disulfide. *Journal of the American Chemical Society, 74*(2), 525-526.

Wagman, D. D., Evans, W. H., Parker, V. B., Schumm, R. H., & Halow, I. (1982). The NBS tables of chemical thermodynamic properties. Selected values for inorganic and C1 and C2 organic substances in SI units: DTIC Document.

Waldbaum, D. R. (1965). Thermodynamic properties of mullite, andalusite, kyanite and sillimanite. *Am Mineral, 50*, 186-195.

Zhu, Z., Jiang, T., Li, G., Guo, Y., & Yang, Y. (2011). Thermodynamics of Reactions Among Al2O3, CaO, SiO2 and Fe2O3 During Roasting Processes.